Remote microwave monitoring of magnetization switching in CoFeB/Ta/CoFeB spin logic device

R Morgunov, G L'Vova, A Talantsev, O Koplak, S. Petit-Watelot, Xavier Devaux, Sylvie Migot, Yuan Lu, S. Mangin

Remote microwave monitoring of magnetization switching in CoFeB/Ta/CoFeB spin logic device

R. Morgunov, G. L'vova, A. Talantsev, O. Koplak, S. Petit-Watelot, X. Devaux, S. Migot, Y. Lu, and S. Mangin

Citation: Appl. Phys. Lett. **110**, 212403 (2017);
View online: https://doi.org/10.1063/1.4984091
View Table of Contents: http://aip.scitation.org/toc/apl/110/21
Published by the American Institute of Physics

Remote microwave monitoring of magnetization switching in CoFeB/Ta/CoFeB spin logic device

R. Morgunov,[1,2,a)] G. L'vova,[1,2] A. Talantsev,[1,2] O. Koplak,[1] S. Petit-Watelot,[3] X. Devaux,[3] S. Migot,[3] Y. Lu,[3] and S. Mangin[3]
[1]*Institute of Problems of Chemical Physics, 142432 Chernogolovka, Russia*
[2]*Tambov State Technical University, 392000 Tambov, Russia*
[3]*Institut Jean Lamour, UMR 7198 CNRS, Université de Lorraine, Nancy 54601, France*

(Received 9 March 2017; accepted 12 May 2017; published online 23 May 2017)

Stable magnetic states of the MgO/CoFeB/Ta/CoFeB/MgO/Ta spin valve as well as transitions between the states were detected by microwave magnetoresistance (MMR) measured in the cavity of an electron spin resonance spectrometer. Advantages of this experimental technique are the possibility to study the orientation dependence of the MMR, the absence of the additional contact/sample interfaces, the wireless control of the spin valves, and the compatibility of the MMR measurements with ferromagnetic resonance experiments. The magnetic field dependence of the first derivation of the microwave absorption allows one to judge about the negative magnetoresistance of the layers and positive interlayer giant magnetoresistance. The obtained experimental results could be used for engineering of the microwave high sensitive sensors available for remote identification of the stable magnetic and logic states of the spin valves needful in medical spintronics to detect biological objects labeled with nanoparticles. *Published by AIP Publishing.*
[http://dx.doi.org/10.1063/1.4984091]

Magnetic multilayered heterostructures based on CoFeB thin films manifest extremely high values of the magnetoresistance up to 600%, providing engineering of the spin logic devices and next generation of sensors.[1,2] Although the CoFeB multilayered heterostructures have been studied for a long time,[3,4] they still evoke increasing scientific interest.[5] One of the basic parameters of the GMR heterostructures is the relative change in DC resistance caused by the reorientation of the magnetization of the ferromagnetic layers.[1–5] Widely adopted measurements of resistance with electrical contacts on the sample surface are very complicate procedures requiring special conditions for contact deposition. This method complicates sensor technology, impedes realization of the remote verification of logic states, and requires masterly microsystem engineering. Even though researchers have developed and are developing various testing schemes, one still can see majority more or less probe the stable/equilibrium GMR sensor state probed under a DC current simultaneously with alternative kinds of methods, including optical monitoring by the Kerr effect[3–5] and AC magnetoimpedance method (*MI*).[6–9] Magnetoimpedance (*MI*) effects in multilayered spin valves, magnetic tunneling junctions, heterostructures manifesting Giant Magneto Resistance (GMR), and ensembles of nanoparticles and nanowires are well known.[6–9] Practical applications of the *MI* are monitoring of GMR sensor switching sensitive to proteins labeled by ferromagnetic nanoparticles (so called medical spintronics).[10,11] The method proposed in our article looks similar to *MI* measurements of the impedance in the magnetic field[6–9] except the high frequency (~10 GHz) microwave field in our work, instead of comparatively low frequencies in the MI experiments limited by the 10–100 MHz range. The advantage of the microwave monitoring proposed in our article is wireless detection of the stable states of the GMR devices and possibility to study anisotropy of their magnetoresistance. Although phenomenological similarity between MI and microwave magnetoresistivity (MMR) takes place, the results obtained in the *X*-band microwave field range in this paper are rather different from MI data mentioned above. In our work, sensors were tested by the 10 GHz microwave magnetic field close to operating frequency in computer memory devices. We will show that microwave magneto resistance (MMR) of the multilayer structure as well as orientations of magnetizations of layers can be monitored by microwave absorption measured in a microwave cavity of an electron spin resonance (ESR) spectrometer. This work is aimed at experimental searching for the correlation between the microwave absorption and the magnetic state switching induced by the external magnetic field. The accurate map of the temperature and field dependent states of the studied spin valve and description of the transitions between stable magnetization states were presented in Ref. 12.

A single ferromagnetic layer system, which consists of MgO(2.5 nm)/CoFeB(1.1 nm)/MgO(2.5 nm)/Ta(5 nm) (sample ***I***), was deposited on the undoped GaAs (001) substrate by magnetron sputtering. The bilayer system, which consists of MgO(2.5 nm)/CoFeB(1.1 nm)/Ta(0.75 nm)/CoFeB(0.8 nm)/MgO(2.5 nm)/Ta(5 nm) (sample ***II***), was deposited on the undoped GaAs (001) substrate (Fig. 1). Scanning transmission electron microscopy (STEM) and energy-dispersive X-ray spectroscopy (EDX) analyses were performed using a probe-corrected JEOL ARM200 operated at 200 kV. The cross-section lamella shown in Fig. 1(a) was prepared using a Focus Ion Beam (FIB) dual beam system (FEI Helios Nanolab 600i). The image reveals continuous and homogeneous layer structures. We can identify the detailed structure of sample and the

[a)]E-mail: morgunov2005@yandex.ru

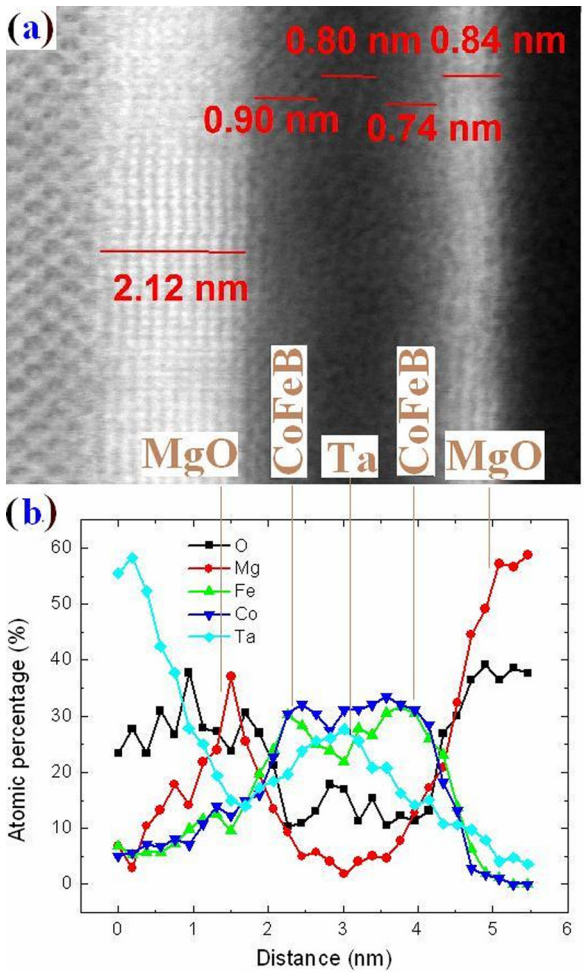

FIG. 1. (a) STEM bright-field image of a cross section of the sample II and (b) EDX profile of sample II.

thickness of each layer from the image contrast. The interface between CoFeB/Ta is quite diffused, which suggests an intermixing or diffusion of Ta in the CoFeB layer after annealing [Fig. 1(a)]. The thickness of the Ta layer was estimated to be 0.88 ± 0.2 nm, which is in agreement with the nominal thickness of 0.75 nm. In addition, EDX analysis was performed to check the chemical distribution of the sample, which is shown in Fig. 1(b). The inset of Fig. 1(b) indicates the position of the line-scan recorded with a spatial resolution of 0.2 nm from the capping layer to the substrate. Interlayer diffusion clearly demonstrated in Fig. 1(b) is the necessary condition for perpendicular anisotropy providing GMR.

The GaAs substrate was selected for easy integration into semiconductor based devices such as spin light emitting diode (LED) structures,[13,14] and for future semiconductor compatible applications in spintronics. Growth conditions are described in detail in Refs. 13 and 14. In the investigated layer stack, the hybridization of the 3d orbitals of transition metals (Co, Fe) with the O_{2p} orbitals of MgO provides perpendicular magnetic anisotropy (PMA) at the CoFeB/MgO interface.[15] To enhance PMA, rapid temperature annealing was performed at 250 °C for 3 min to crystallize the CoFeB layer. During this process, diffusing boron was absorbed by the 0.75 nm Ta interlayer, which also provided antiferromagnetic coupling between the two adjacent CoFeB layers.[13,14] To identify the switching sequence for bottom and top CoFeB layers from *M–H* curves, we performed the spin-LED measurement sensitive to the magnetization state of the bottom CoFeB layer only. In addition, the total magnetic dead layer is determined to be about 0.5 nm, which is almost equally distributed in both sides of the Ta insertion layer.[13] The plate-shaped sample $0.4 \times 4 \times 4\,mm^3$ in size was studied in experiments.

Both microwave magnetoresistance (MMR) and ferromagnetic resonance (FMR) signals were recorded using a Bruker ESP 300 X-band ESR spectrometer (microwave frequency: $f_0 = 9447$ GHz, microwave power: 6.3 mW, modulation frequency: 100 kHz, modulation amplitude: 10 Oe, and quality factor: $Q \sim 4000$). Orientation of the sample in the microwave cavity is shown in Figs. S1(a) and S1(b). If the resistance of the sample ρ is lower than the resistance of the microwave circuit ($R_C \sim 190\,\Omega$), absorbed microwave power P is proportional to sample resistance and depends on magnetic field $P \sim \rho(H)$.[16,17] (See detailed description of the method of MMR measurements in the supplementary material). Thus, in our experiments, the derivation of absorbed microwave power measured by the modulation method was directly proportional to the derivation of sample resistance $dP/dH \sim d(\rho(H))/dH$. Magnetic hysteresis loops were obtained with an MPMS 5XL Quantum Design superconducting quantum interference device (SQUID) magnetometer.

Nonresonant absorption of microwave power was measured at $T = 300$ K in the range of the DC field from -1000 Oe to $+1000$ Oe in the direct and backward sweeping modes [Figs. 2(a) and 3(a)]. These measurements were accompanied by recording the hysteresis loops in the SQUID magnetometer [Figs. 2(b) and 3(b)]. The decrease in the magnetic field (backward magnetic field sweeping) results in dP/dH peculiarities in negative and positive fields close to saturation field values of the single ferromagnetic layer (sample ***I***) [Figs. 2(a) and 2(b)]. In bilayer (sample ***II***), dependence $dP/dH(H)$ contains three sharp jumps [Fig. 3(a)] in magnetic fields $+200$ Oe, -25 Oe, and -230 Oe, close to the critical transition fields of the tilting of layer magnetization determined using a SQUID magnetometer [Fig. 3(b)]. Jumps of the dP/dH value in magnetic fields $+200$ Oe and -230 Oe corresponding to transitions accompanied by magnetization tilting of one of the two ferromagnetic layers were about two times smaller than dP/dH jump amplitude in magnetic field -25 Oe corresponding to transition accompanied by magnetization tilting of both ferromagnetic layers.

The slope $k_1 = d^2P/dH^2(H) = 1 \times 10^{-2}$ a.u./Oe of the $dP/dH(H)$ dependence between transitions at 200 Oe and -25 Oe and the slope of the dependence between transitions at -25 Oe and -230 Oe (magnetizations of the ferromagnetic layers in these intervals are opposite to each other) are two times larger than the slope $k_2 = 5 \times 10^{-3}$ a.u./Oe of the $dP/dH(H)$ curve in the rest intervals (at $H > 200$ Oe and $H < -230$ Oe), where magnetizations of the layers are directed in the same way.

Dependence $dP/dH(H)$ recorded in the upward sweeping direction has the same slopes k_1 and k_2 of the corresponding parts and contains three transitions in magnetic fields -200 Oe, $+25$ Oe, and $+230$ Oe. Two dependences $dP/dH(H)$ recorded in upward and backward sweeping modes form complicated hysteresis loops [Fig. 3(a)] similar to the

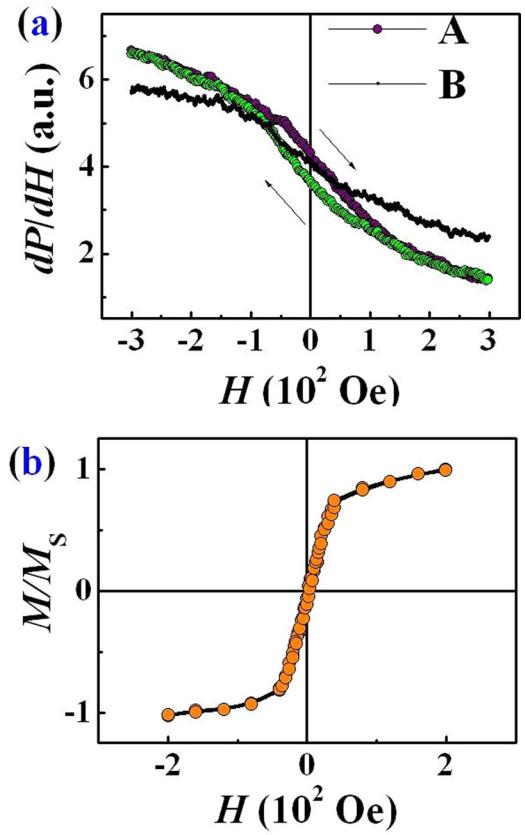

FIG. 2. (a) Field dependences of the first derivation of microwave absorption dP/dH(H) in the single layer (sample I) for the upward and backward magnetic field H sweeping at temperature T = 300 K, for two different orientations of the magnetic field with respect to the sample plane: configuration A corresponds to 0° and configuration B corresponds to 90°. (b) Magnetic hysteresis loops recorded in a SQUID magnetometer for single layer (sample I) and at T = 300 K.

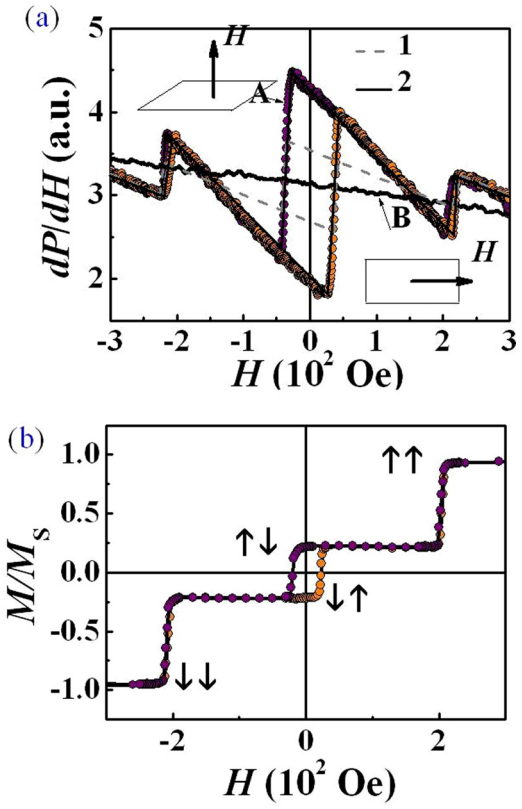

FIG. 3. (a) Field dependences of the first derivation of microwave absorption dP/dH(H) in the bilayer (sample II) for the upward and backward magnetic field H sweeping at temperature T = 300 K, for two different orientations of the magnetic field with respect to the sample plane: configuration A corresponds to 0° and configuration B corresponds to 90°. Modelling of the hysteresis loop of the dP/dH(H) with no interlayer TMR is shown by dashed line 1. Solid line 2 is theoretical hysteresis loop dP/dH(H) assuming contribution of the TMR. (b) Magnetic hysteresis loops recorded in the SQUID magnetometer for the double layer (sample II) at T = 300 K. Arrows show magnetization directions of the bottom layer (left arrow) and upper layer (right arrow).

hysteresis of magnetic moment [Fig. 3(b)] containing one inner loop centered at the zero field (~25 Oe coercive field) and two outer loops centered at ±215 Oe (coercive fields ~15 Oe).

The *P(H)* dependences obtained by integration of the *dP/dH(H)* dependences [Figs. 2(a) and 2(b)] are presented in Figs. S2(a) and S2(b). The angular dependence of the *dP/dH(H)* and its hysteresis loop parameters are given in supplementary material Figs. S3(a) and S3(b). All the above described data are related to the low magnetic fields below 2 kOe. In high fields close to 3.4 kOe corresponding to *g*-factor $g \sim 2$, ferromagnetic resonance (FMR) can be excited in samples ***I*** and ***II***, the crossed sweeping and microwave magnetic fields [see supplementary material Figs. S4(a) and S4(b)]. Anisotropy of resonant field H_{res} and line width of the FMR lines $H_{p\text{-}p}$ in samples ***I*** and ***II*** are discussed in the supplementary material [Figs. S5(a) and S5(b)].

One of the common types of MMR is positive Lorentz magnetoresistance caused by shortening of charge carriers trajectories in the magnetic field.[18] In that case, the slope of the *dP/dH(H)* dependence is proportional to magnetic field $B = H + 4\pi M$, which is proportional to *H* when there is no abrupt change in the sample magnetization. The GMR effect results in additional coefficient α in front of *H* ($dP/dH \sim \alpha H$) and does not change the sign of the slope. Therefore, the combination of the positive Lorentz magnetoresistance with GMR may result in the positive slope of *dP/dH(H)* only, which is in contrast to our experiment. The *dP/dH(H)* slopes [Figs. 2(a) and 3(a)] corresponding to stable magnetic states [Figs. 2(b) and 3(b)] are demonstrated to be negative for all gradual regions of *dP/dH* vs *H* curves for samples ***I*** and ***II*** (narrow sectors of the *dP/dH(H)* curve with positive slopes correspond to transitions between stable states).

In our experiments, decreasing linear dependence $dP/dH(H) \sim d\rho/dH \sim -H$ indicates negative MMR quadratic dependence on magnetic field $\rho(H) \sim -H^2$, $d\rho/dH \sim -H$. One can propose few different types of the MMR corresponding to the above mentioned field dependence. In low dimensional systems, summation of the amplitudes of the electronic probabilities along their trajectories results in different amounts of closed and open electronic orbits in the presence and in the absence of the external magnetic field.[19] Since open orbits contribute to conductivity, negative MMR satisfies the condition $\rho(H) \sim -H^2$. The same dependence can be found due to spin-dependent scattering of charge carriers by magnetic inclusions (doping atoms, ferromagnetic clusters, etc.).[20] More or less realistic explanation of the origin of MMR is changes in the large minority density of state (DOS) of CoFe-O above the Fermi level.[21–23] In Ref. 6, the theory of the *AC* spin-valve effect in symmetric tunneling magnetoresistance (TMR)

junctions and prediction of negative *AC* magnetoresistance due to resonant amplification and depletion of the spin accumulation were proposed. Negative magnetoresistance resulting from the interplay of the diffusion and spin relaxation times of the charge carriers appears in the GHz frequency range similar to our experimental data.[6]

Assuming one of the mentioned mechanisms of the negative MMR, one can propose the explanation of the hysteresis of the $dP/dH(H)$ dependence. First, the single ferromagnetic layer (sample ***I***) should be considered in the magnetic field with the help of known equality $\boldsymbol{B = H + 4\pi M}$ binding magnetic induction $\boldsymbol{B}$ and field strength $\boldsymbol{H}$.[24] The magnetic field inside the layer $B_{01} = H + 4\pi M$ is determined as a sum of external magnetic field H and layer magnetization $4\pi M$.[24] The increase in the external magnetic field directed opposite to the layer magnetization causes tilting of the magnetic moment, and changed induction of the magnetic field $B_{02} = H - 4\pi M$ is stabilized in the layer. The change in the magnetic induction accompanying the jumps is $\Delta B = 8\pi M$ (if one neglects a small change of H during the magnetization jump). Since MMR is controlled by internal magnetic field induction $\rho(B) \sim -B^2$, a change in the B value caused by magnetization tilting initiates jump of the resistivity $\Delta\rho(B) \sim -((B_{02})^2 - (B_{01})^2) = 16\ \pi MH$. The derivation of the resistivity is also manifesting jump $\Delta(d\rho(B)/dB) \sim M$. The gradually changing magnetization contributing to the dP/dH led to different slopes corresponding to the two ends of the $dP/dH(H)$ curve. Experimental evidence of this fact for the single layer is the hysteresis of the dP/dH value [Fig. 2(a)] corresponding to hysteresis of the sample magnetization [Fig. 2(b)].

Now the bilayer system (sample ***II***) should be considered. Similar to the single layer, the resistance of the each layer is quadratically proportional to the magnetic field induction inside the layer $\rho_1(B) \sim -B_1^2$, $\rho_2(B) \sim -B_2^2$. Index $\langle\langle 1\rangle\rangle$ corresponds to the thick layer; and index $\langle\langle 2\rangle\rangle$ corresponds to the thin layer. Scattering magnetic fields can be neglected because they exist near the films edges and the ratio of the sample thickness to the linear film size is very small $\sim 10^{-6}$. Four modes of the dP/dH behavior are possible depending on mutual orientations of the two ferromagnetic layers accordingly with four configurations sketched by arrows in Fig. 3(b). The corresponding dP/dH values can be expressed by summarizing the contributions $(dP/dH)_1 \sim B_1$ and $(dP/dH)_2 \sim B_2$ of each layer taking into account signs of their magnetization vectors and direction of full sample magnetization with respect to the external magnetic field

$$\begin{aligned}
(dP/dH)_{\uparrow\uparrow} &= (dP/dH)_1 + (dP/dH)_2 \sim -B_1 - B_2 \\
&= -2H + 4\pi\,(M_1 + M_2), \\
(dP/dH)_{\uparrow\downarrow} &\sim -2H + 4\pi(M_1 - M_2), \\
(dP/dH)_{\downarrow\uparrow} &\sim -2H - 4\pi\,(M_1 - M_2), \\
(dP/dH)_{\downarrow\downarrow} &\sim -2H - 4\pi(M_1 + M_2). \qquad (1)
\end{aligned}$$

The arrow direction indexing $(dP/dH)_{\uparrow\downarrow}$ corresponds to orientations of the layers magnetizations with respect to the positive direction of the external magnetic field H. The left arrow corresponds to magnetization of the thick layer, while the right arrow corresponds to magnetization of the thin layer. The change in the dP/dH value initiated by transitions between four magnetic states of the bilayer sample is controlled by the following expressions obtained by subtraction of the corresponding expressions (1) from each other:

$$\begin{aligned}
\Delta(dP/dH)_{\uparrow\uparrow\leftrightarrow\uparrow\downarrow} &= \Delta(dP/dH)_{\downarrow\uparrow\leftrightarrow\downarrow\downarrow} \sim -2H + 4\pi(M_1 + M_2) - (-2H + 4\pi(M_1 - M_2)) \\
&= 8\pi M_2 = 4.8\,\text{kG}, \\
\Delta(dP/dH)_{\uparrow\downarrow\leftrightarrow\downarrow\uparrow} &\sim -2H + 4\pi(M_1 - M_2) - (-2H - 4\pi\,(M_1 - M_2)) \\
&= 8\pi\,(M_1 - M_2) = 9.4\,\text{kG} \\
\Delta(dP/dH)_{\uparrow\uparrow\leftrightarrow\downarrow\downarrow} &\sim -2H + 4\pi(M_1 + M_2) - (-2H - 4\pi(M_1 - M_2)) \\
&= 8\pi(M_1 + M_2) = 19\,\text{kG}. \qquad (2)
\end{aligned}$$

Details of numerical calculations are presented in the supplementary material. Expressions (2) allow us to conclude that the maximal change in the derivation of the microwave absorption should be observed due to simultaneous tilting of magnetizations of both ferromagnetic layers [see theoretical dependence $dP/dH(H)$ in Fig. 3(a), dashed curve 1]. Good coincidence of the theoretical predictions and experimental results is evidence of that the dP/dH hysteresis originates from negative MMR manifesting quadratic field dependence. Thus, inner and outer hysteresis loops on the $dP/dH(H)$ dependence as well as the ratio of the inner and outer loops amplitudes are explained by drop changes in negative MMR of the bilayer system caused by transitions between its magnetic and logic states.

The slope k_1 of the $dP/dH(H)$ dependence in $\uparrow\downarrow$ and $\downarrow\uparrow$ antiparallel states is different from the slope k_2 in the $\uparrow\uparrow$ and $\downarrow\downarrow$ parallel states. This fact cannot be explained by negative MMR only. Together with negative MMR, the positive MMR contribution corresponding to interlayer spin-dependent electron tunneling (GMR) should be taken into account. If one assumes GMR, expressions (1) should be rewritten as

$$\begin{aligned}
(dP/dH)_{\uparrow\uparrow} &\sim -2H + 4\pi(M_1 + M_2), \\
(dP/dH)_{\uparrow\downarrow} &\sim \alpha(-2H + 4\pi(M_1 - M_2)), \\
(dP/dH)_{\downarrow\uparrow} &\sim \alpha(-2H - 4\pi(M_1 - M_2)), \\
(dP/dH)_{\downarrow\downarrow} &\sim -2H - 4\pi(M_1 + M_2). \qquad (3)
\end{aligned}$$

Here, α is the GMR coefficient. In our experiments, $(dP/dH)_{\uparrow\downarrow} \sim 2(dP/dH)_{\uparrow\uparrow}$ (see theoretical dependence $dP/dH(H)$ in Fig. 3, solid curve 2), i.e., the value of the positive GMR in the bilayer sample is about ~100%, which is in good agreement with our results of direct measurements of the GMR by the galvanic four probe method in the CIP (Conductivity In Plane) configuration.

Contributions of the negative MMR of the each layer and positive GMR of the bilayered MgO/CoFeB/Ta/CoFeB/MgO/Ta sample to the field dependence of the derivation of the microwave absorption power were distinguished. Amplitude of the derivation jumps caused by magnetization tilting is controlled by negative MMR, while the ratio between the slopes of the (dP/dH) (H) dependences is determined by positive GMR.

Experimental data confirm in a technically unique way that the microwave magnetoresistance (MMR), and dP/dH the field derivative of the microwave absorption, can be correlated with magnetic switching of the spin valve verified by the DC measurement through the SQUID magnetometer. The key notion tested in the reported experiments is the behaviour of a dP/dH value in the sweeping magnetic field. The microwave field drove the stable magnetic state, at a specific H field on the M-H curve, out of balance a little bit in order to probe the magnetic state. It is pretty straightforward to see that the response of dP/dH is naturally correlated with the $M(H)$ curve. The obtained results allow development of the contactless remote technique for identification of the spin valve logic states and threshold interstate switching magnetic fields. The significance of these research studies is to develop a method for the remote monitoring of the GMR sensors by microwave irradiation.

See supplementary material for the technique of MMR measurements and complete ESR data including resonant signals of single and double layered samples.

This work was supported by the Ministry of Education and Science of Russian Federation (Grant No. 3.1992.2017/PCh), joint French National Research Agency (ANR)-National Natural Science Foundation of China (NSFC) SISTER project (Grants Nos. ANR-11-IS10-0001 and NNSFC 61161130527), and ENSEMBLE project (Grant Nos. ANR-14-0028-01 and NNSFC 61411136001) as well as by Région Lorraine, ANR-NSF Project, ANR-13-IS04-0008-01, COMAG by the ANR-Labcom Project LSTNM, and by the Université de la Grande Region.

[1]S. Ikeda, J. Hayakawa, Y. Ashizawa, Y. M. Lee, K. Miura, H. Hasegawa, M. Tsunoda, F. Matsukura, and H. Ohno, Appl. Phys. Lett. **93**, 082508 (2008).
[2]S. S. P. Parkin, C. Kaiser, A. Panchula, P. M. Rice, B. Hughes, M. Samant, and S. Yang, Nat. Mater. **3**, 862 (2004).
[3]C. Reig, S. Cardoso, and S. Mukhopadhyay, in *Giant Magnetoresistance (GMR) Sensors from Basis to State-of-the-Art Applications*, edited by S. Mukhopadhyay (Springer-Verlag, New York, 2013), pp. 103–131.
[4]I. Žutic, J. Fabian, and S. Das Sarma, Rev. Mod. Phys. **76**, 323 (2004).
[5]D. Lee, T.-H. Shim, and J.-G. Park, Nanotechnology **27**, 295705 (2016).
[6]D. Kochan, M. Gmitra, and J. Fabian, Phys. Rev. Lett. **107**, 176604 (2011).
[7]S. Ingvarsson, M. Arikan, M. Carter, W. Shen, and G. Xiao, Appl. Phys. Lett. **96**, 232506 (2010).
[8]D. Garcia, J. L. Munoz, G. Kurlyandskaya, M. Vazquez, M. Ali, and M. R. J. Gibbs, J. Magn. Magn. Mater. **191**, 339 (1999).
[9]W. C. Chien, C. K. Lo, L. C. Hsieh, Y. D. Yao, X. F. Han, Z. M. Zeng, T. Y. Peng, and P. Lin, Appl. Phys. Lett. **89**, 202515 (2006).
[10]A. V. Silva, D. C. Leitao, J. Valadeiro, J. Amaral, P. P. Freitas, and S. Cardoso, Eur. Phys. J: Appl. Phys. **72**, 10601 (2015).
[11]T. Zhu, P. Chen, Q. H. Zhang, R. C. Yu, and B. G. Liu, Appl. Phys. Lett. **104**, 202404 (2014).
[12]O. Koplak, A. Talantsev, A. Hamadeh, P. Pirro, T. Hauet, R. Morgunov, and S. Mangin, J. Magn. Magn. Mater. **433**, 91 (2017).
[13]B. S. Tao, P. Barate, J. Frougier, P. Renucci, B. Xu, A. Djeffal, H. Jaffès, J.-M. George, X. Marie, S. Petit-Watelot, S. Mangin, X. F. Han, Z. G. Wang, and Y. Lu, Appl. Phys. Lett. **108**, 152404 (2016).
[14]S. H. Liang, T. T. Zhang, P. Barate, J. Frougier, M. Vidal, P. Renucci, B. Xu, H. Jaffrès, J. M. George, X. Devaux, M. Hehn, X. Marie, S. Mangin, H. X. Yang, A. Hallal, M. Chshiev, T. Amand, H. F. Liu, D. P. Liu, X. F. Han, Z. G. Wang, and Y. Lu, Phys. Rev. B **90**, 085310 (2014).
[15]H. X. Yang, M. Chshiev, B. Dieny, J. Lee, A. Manchon, and K. Shin, Phys. Rev. B **84**, 0544101 (2011).
[16]A. I. Veinger, A. G. Zabrodskii, and T. V. Tisnek, Phys. Status Solidi B **230**, 107 (2002).
[17]R. Morgunov, M. Farle, M. Passacantando, L. Ottaviano, and O. Kazakova, Phys. Rev. B **78**, 045206 (2008).
[18]A. B. Pippard, *Magnetoresistance in Metals* (Cambridge University Press, 1989).
[19]B. L. Altshuler and A. G. Aronov, "Modern problems in condensed matter sciences," in *Electron–Electron Interaction in Disordered Systems* edited by V. M. Agranovich and A. A. Maradudin (North-Holland Publishing, Amsterdam, 1985), Vol. **10**.
[20]B. I. Shklovskii and B. Z. Spivak, in *Hopping Transport in Solids*, edited by M. Pollak and B. Shklovskii (Elsevier, Amsterdam, 1991), p. 271.
[21]F. Greullet, E. Snoeck, C. Tiusan, M. Hehn, D. Lacour, O. Lenoble, C. Magen, and L. Calmels, Appl. Phys. Lett. **92**, 053508 (2008).
[22]M. Sharma, S. X. Wang, and J. H. Nickel, Phys. Rev. Lett. **82**, 616 (1999).
[23]L. X. Jiang, H. Naganuma, M. Oogane, K. Fujiwara, T. Miyazaki, K. Sato, T. J. Konno, S. Mizukami, and Y. Ando1, J. Phys.: Conf. Ser. **200**, 052009 (2010).
[24]C. Kittel, *Introduction to Solid State Physics*, 8th ed. (Wiley, 2004), p. 704.